

Electronic supplementary information

Highly efficient and thermally stable broadband near-infrared emitting garnet $\text{Ca}_3\text{Sc}_2\text{Ge}_3\text{O}_{12}:\text{Cr}^{3+}$, Ce^{3+} for multiple pc-LED applications

Yining Wang,^a Mengmeng Shang,^{*a} Yixin Sun,^a Minliang Deng,^a Xiaole Xing,^a

Peipei Dang,^b and Jun Lin^{*b}

a. Key Laboratory for Liquid-Solid Structural Evolution and Processing of Materials (Ministry of Education), School of Material Science and Engineering, Shandong University, Jinan 250061, P.

R. China

b. State Key Laboratory of Rare Earth Resource Utilization, Changchun Institute of Applied

Chemistry, Chinese Academy of Sciences, Changchun 130022, P. R. China

Corresponding author:

*Mengmeng Shang, Email: mmshang@sdu.edu.cn

*Jun Lin, Email: jlin@ciac.ac.cn

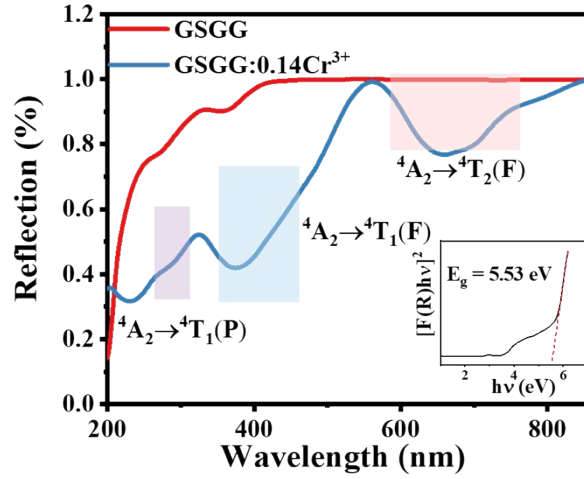


Fig. S1 Diffuse reflectance spectra (DRS) of CSGG: $x\text{Cr}^{3+}$ ($x = 0, 0.14$).

(1) The band gap (E_g) values of the host can be evaluated by the Kubelka-Munk equations:

$$F(R) = (1 - R)^2/2R \quad (S1)$$

$$[F(R) \times hv]^2 = A(hv - E_g) \quad (S2)$$

where $F(R)$ represents the absorption, R is the reflectance (%), and $h\nu$ is the incident photon energy, A is a constant, E_g is the bandgap value. Based on the DRS, the E_g values of CSGG hosts were determined to be 5.53 eV.

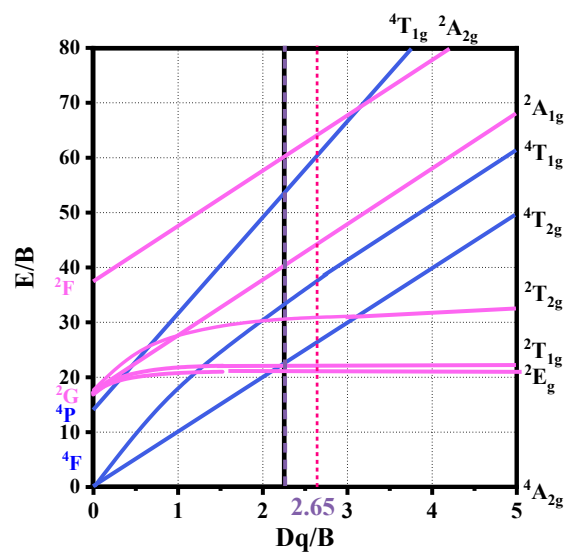


Fig. S2 Tanabe-Sugano diagram for a Cr³⁺ ion in octahedral coordination. Dq/B value of Cr³⁺ in GSGG are marked in the Figure.

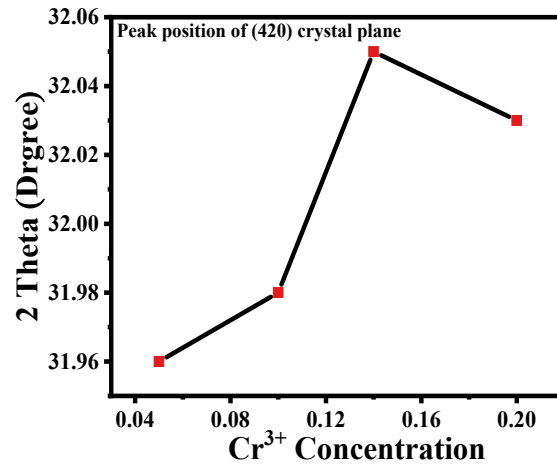


Fig. S3 Variation of the shift of the diffraction peak on the (420) crystal plane with increasing doping of Cr³⁺.

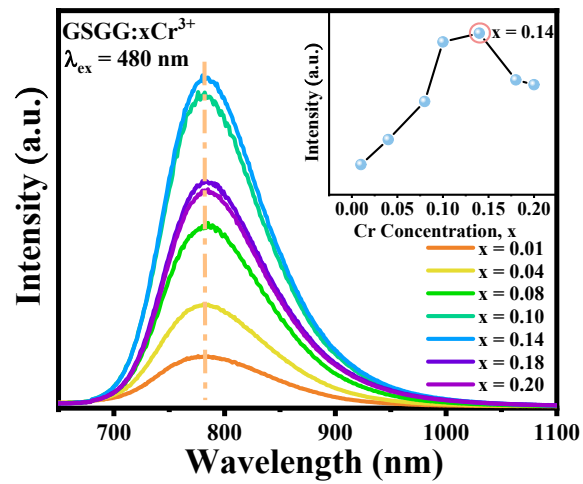


Fig. S4 Concentration-dependent emission spectra of CSGG:xCr³⁺ (x = 0.01, 0.04, 0.08, 0.10, 0.14, 0.18, 0.20) phosphors. The upper inset shows the integral emission intensity under different Cr³⁺ doping concentrations.

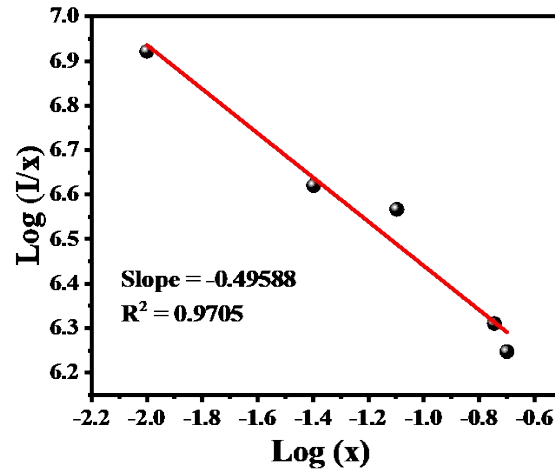


Fig. S5 Relationship between $\log (I/x)$ and $\log x$ of GSGG:xCr³⁺.

The mechanism can be obtained using the following formula:

$$\log \left(\frac{I}{x} \right) = A - \frac{\theta}{3} \log x$$

Where I is the emission intensity, x is the concentration of the activator ions above the quenching concentration, β and K are constant for the same excitation conditions. The $\theta = 3$ represents the interaction type of the energy transfer between the nearest-neighbor ions, while $\theta = 6, 8,$ and 10 represent dipole-dipole, dipole-quadrupole, and quadrupole-quadrupole interactions, respectively.

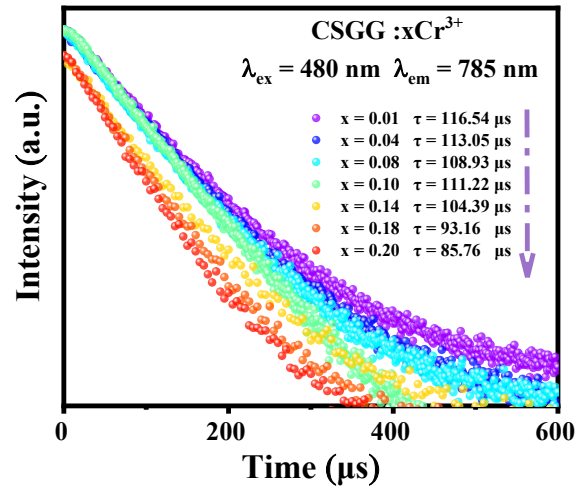


Fig. S6 Decay curves of CSGG:xCr³⁺ phosphor under different Cr³⁺ doping concentrations.

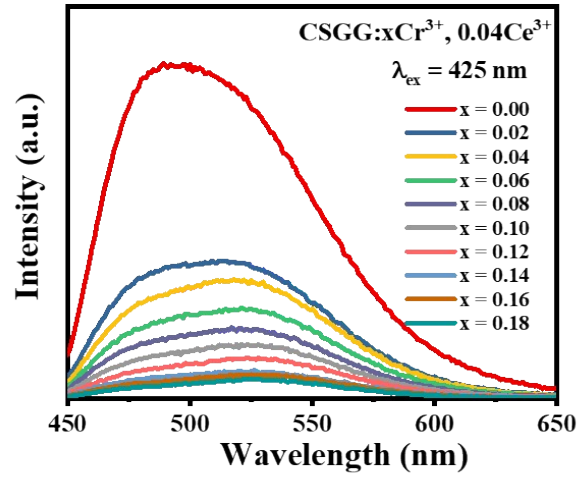


Fig. S7 The emission spectra of CSGG: $x\text{Cr}^{3+}$, 0.04Ce^{3+} ($x = 0-0.18$) in the NIR range.

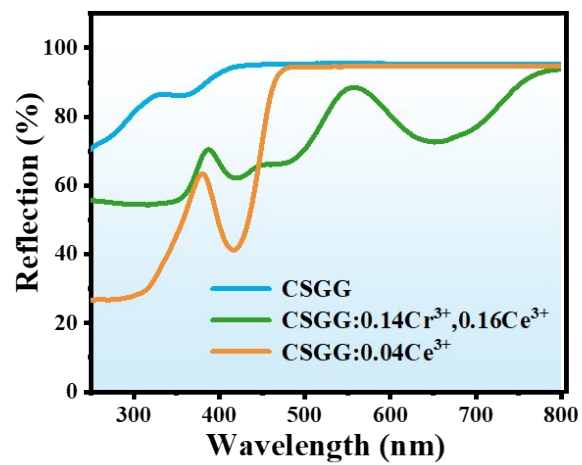


Fig. S8 DRS of CSGG host, CSGG:0.14Cr³⁺, 0.16Ce³⁺, and CSGG:0.04Ce³⁺.

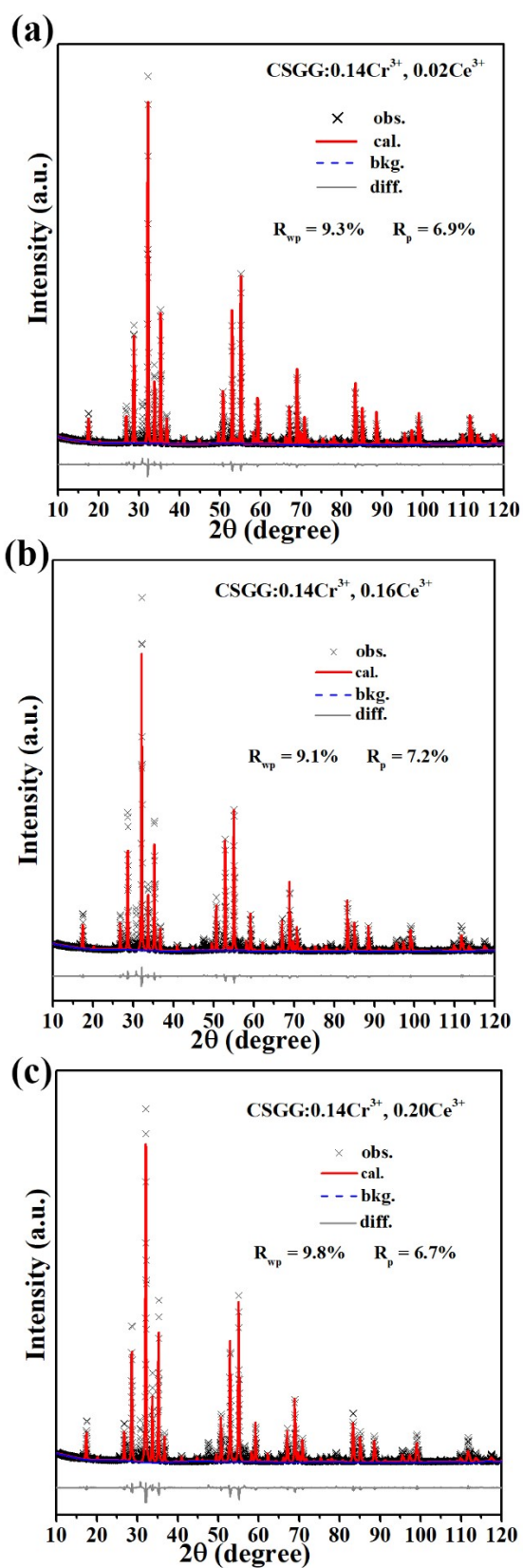


Fig. S9 XRD Rietveld refinement of (a) CSGG:0.14Cr³⁺, 0.02Ce³⁺, (b) CSGG:0.14Cr³⁺, 0.16Ce³⁺, and (c) CSGG:0.14Cr³⁺, 0.20Ce³⁺.

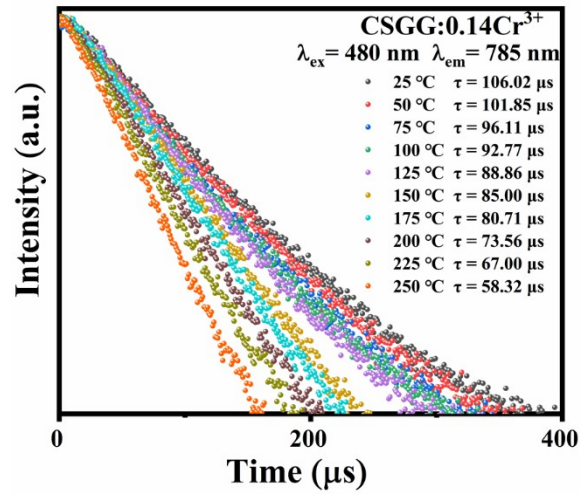


Fig. S10 Decay curves of CSGG:0.14Cr³⁺ phosphors at different temperatures.

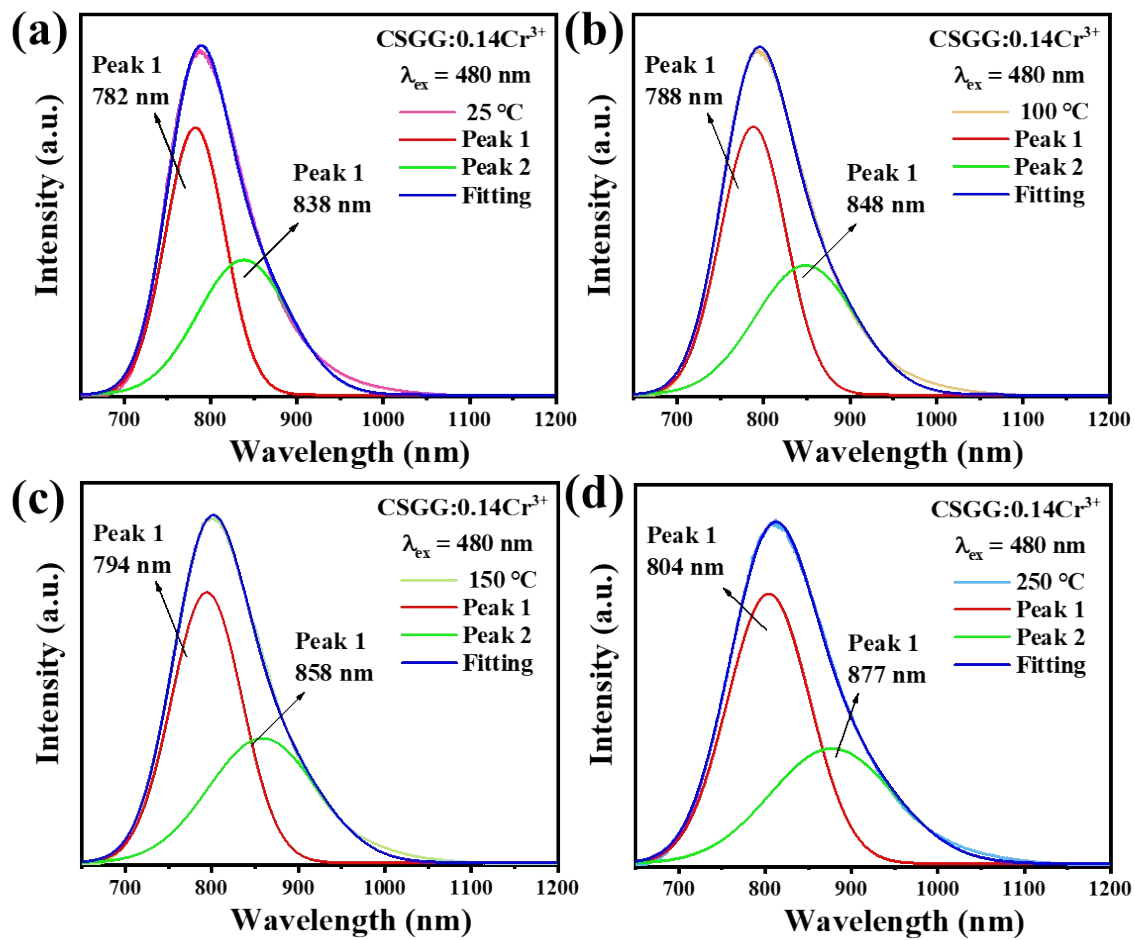


Fig. S11 The PL spectrum and corresponding Gaussian fitting of CSGG:0.14Cr³⁺ phosphor recorded at (a) 25 °C, (b) 100 °C, (c) 150 °C, and (d) 250 °C.

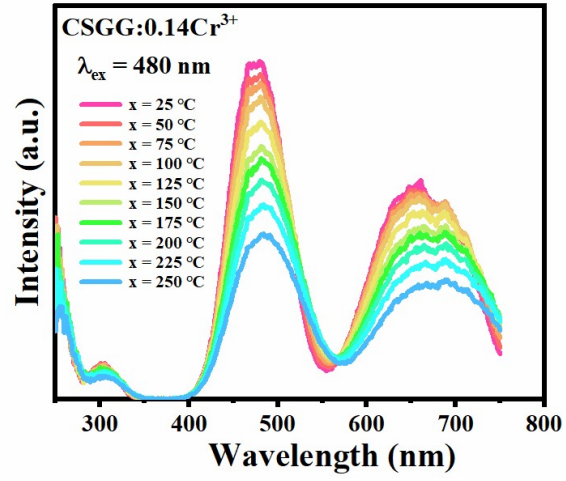


Fig. S12 Temperature-dependent excitation spectra of CSGG:0.14Cr³⁺.

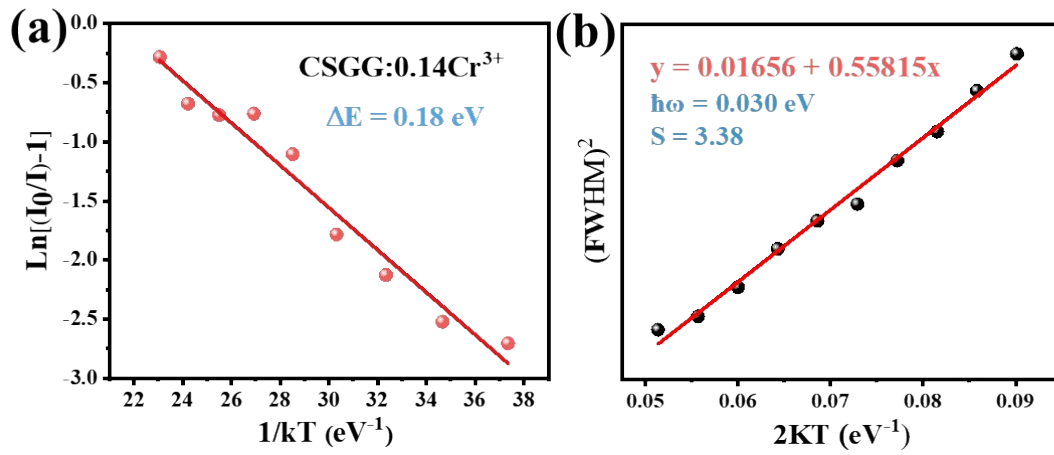


Fig. S13 (a) Variable temperature spectra of $\text{Ln}[(I_0/I)-1]$ versus $1/kT$ were plotted.

(b) Fitting FWHM curve with temperature.

Table S1 Main parameters of processing and refinement results of CSGG:0.14Cr³⁺, yCe³⁺ (y = 0.02, 0.16, 0.20).

CSGG:Cr ³⁺	y = 0.02	y=0.16	y = 0.20
Space group	<i>Ia3d</i>	<i>Ia3d</i>	<i>Ia3d</i>
<i>a</i> = <i>b</i> = <i>c</i> , Å	12.500594(235)	12.502334(264)	12.506791(160)
<i>V</i> , Å ³	1953.403(110)	1954.219(124)	1956.310(75)
$\alpha = \beta = \gamma$	90°	90°	90°
R _{wp} , %	9.3	9.1	9.8
R _p , %	6.9	7.2	6.7
χ^2	2.401	2.386	2.391

Table S2. Selected bond length (Å) of CSGG:0.14Cr³⁺, yCe³⁺ (y = 0.02, 0.16, 0.20).

	y = 0.02	y = 0.16	y = 0.20
8×Ca—O	4×2.4370 (2)	4×2.42306 (4)	4×2.40094 (4)
	4×2.50086 (5)	4×2.50684 (3)	4×2.51506 (5)
Average bond length	2.47192	2.46495	2.45800
<i>D</i> *	1.41%	1.70%	2.32%

(*lattice distortion index $D = \frac{1}{n} \frac{\sum_{i=1}^n |d_{av} - d_i|}{d_{av}}$)